Stacked 2D Crystalline Sheets of the Membrane-Protein Bacteriorhodopsin: A Specular and Diffuse Reflectivity Study

I. Koltover,[1] T. Salditt,[1,*] J.-L. Rigaud,[2] and C. R. Safinya[1]
[1]*Materials Department, Physics Department, and Biochemistry and Molecular Biology Program, University of California, Santa Barbara, California 93106*
[2]*Institut Curie, Section de Recherche, Paris, France*
(Received 18 May 1998)

We report a specular and diffuse x-ray reflectivity study of a model multilayer membrane-protein system. Native membranes containing two-dimensional crystals of the membrane-protein bacteriorhodopsin were fused into giant (10 μm) single-crystalline patches and stacked to form perfect orientationally aligned multilayers. The diffuse scattering indicates a conformal buckling of the membranes on length scales of a few hundred angstroms. Analysis of the truncation rods allows us to elucidate the intermembrane correlations of the proteins at different hydration levels of the multilayer. [S0031-9007(98)07168-3]

PACS numbers: 87.15.By, 61.10.Kw, 61.30.Eb

Integral membrane proteins are critical for a broad range of biological functions such as nerve conduction, energy conversion, transport across cellular membranes, and molecular recognition [1,2]. Aside from the inherent biological interest in the relationship between their structure and function, they are increasingly explored in biotechnology applications [3,4]. Unfortunately, x-ray diffraction studies of membrane protein structure and interactions are rare, due to the difficulty of preparing three-dimensional (3D) crystals of these molecules. Moreover, membrane proteins can affect the structural conformation of their host membranes, making them drastically different from the well-understood model pure lipid bilayers [5].

It is often possible to prepare suspensions of the native cellular membrane multilayers preserving their protein content for low-angle x-ray diffraction study. In these preparations the measured x-ray intensity originates from randomly oriented patches, which limits the extraction of structural parameters. For example, the ability to produce perfectly aligned freely suspended films of lipid membrane multilayers has led to the discovery that the well-known L'_β gel phase in fact consists of three distinct phases [6]. Recently, there has been much success in the development of interface-sensitive x-ray diffraction techniques for the characterization of thin oriented films and multilayers. Application of these techniques to multilayers of protein-rich biological membranes would allow studies of structure and intermolecular interactions in these systems without the complete prior knowledge of their constituting components.

In this work we apply powerful interface-sensitive x-ray scattering techniques to study highly aligned multilayers containing the membrane protein bacteriorhodopsin. We were able to fuse the small 0.5 μm patches of native bacterial membranes to 10 μm size, thus increasing their area 400 times [7]. These giant crystalline membranes were used to prepare high quality multilayers suitable for the application of reflectivity and grazing incidence diffraction techniques. We demonstrate that these techniques reveal a wealth of structural features, in particular regarding the protein-induced membrane conformation on mesoscopic length scales.

Bacteriorhodopsin (bR) is a light-driven proton pump, and a part of the photosynthetic apparatus of the archaebacterium *Halobacterium salinarium*. It is possible to purify bR-rich parts of the native bacterial membrane, the purple membrane (PM), which have $\sim$0.5 μm diameter. These membranes consist of bR trimers ordered in crystalline hexagonal arrays with native lipid species filling the remaining space [7] (Fig. 1). The lipid chains are methylated and do not order at physiological temperatures [8].

Suspensions of the native bacterial purple membrane appear as clumps of small membrane patches when viewed with an optical microscope [Fig. 1(a)]. These

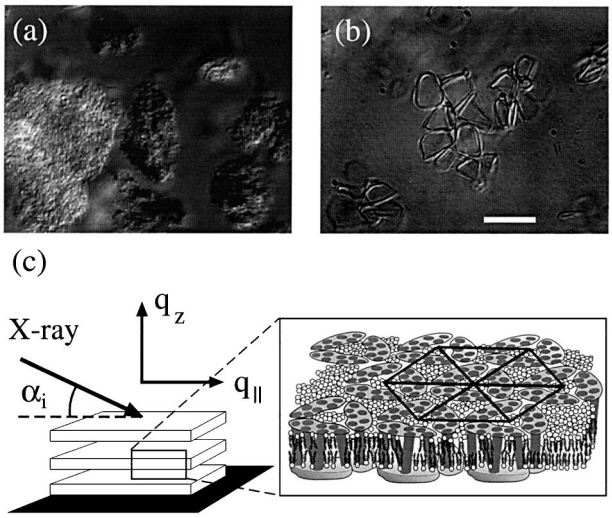

FIG. 1. Differential interference contrast (DIC) optical micrographs of (a) a clump of native PM patches and (b) giant fused patches on the same scale (bar = 10 μm); (c) schematic of the purple membrane multilayer and the experimental geometry.

 0031-9007/98/81(12)/2494(4)$15.00

preparations were extensively washed and resuspended at 3 mg/ml in 0.1 M phosphate buffer (pH5.2). Following a procedure similar to Ref. [7], we achieved fusion of the native PM's by adding two detergents to the buffer: 6 mM octil glucoside (Boehringer) and 200 μM dodecyl-trimethyl ammonium chloride (Kodak). This led to the formation of giant ($\geq$10 μM diameter) fused single-crystalline membranes [Fig. 1(b)], which are extremely flat microscopically, as determined by reflection interference contrast microscopy. To prepare samples for x-ray measurements, the fused PM patches were dialized against a large volume of water to remove any traces of detergent. A 10 μl drop of 0.02 mg/ml PM suspension was deposited on a cleaned hydrophilic surface of a polished silicon wafer. This procedure yielded very thin (1 μm thick = 100–200 membrane layers) highly oriented multilayer films of $\approx$10 mm^2 total area used for the experiments.

Synchrotron x-ray experiments were conducted at the Stanford Synchrotron Radiation Laboratory. We used a standard 4-circle diffractometer with a special environmental chamber which allowed us to control the sample humidity in an inert He atmosphere. The spectrometer resolution was 1.4×10^{-3} rad and 4.2×10^{-3} rad in and out of the plane of incidence, respectively.

Figure 2 shows the reflectivity profiles of a dehydrated bR film and a rocking scan at $\alpha_i + \alpha_f = 1.2°$. In contrast to most multilayer preparations of biological membranes, where a typical mosaic spread of layer orientations is of order 5–10° in the best samples, the mosaicity of our samples is less than 0.04° (Fig. 2). Apart from the sharp central specular peak, the rocking scan shows a considerable amount of diffuse (nonspecular) scattering, modulated by the x-ray optical effects, such as the Yoneda

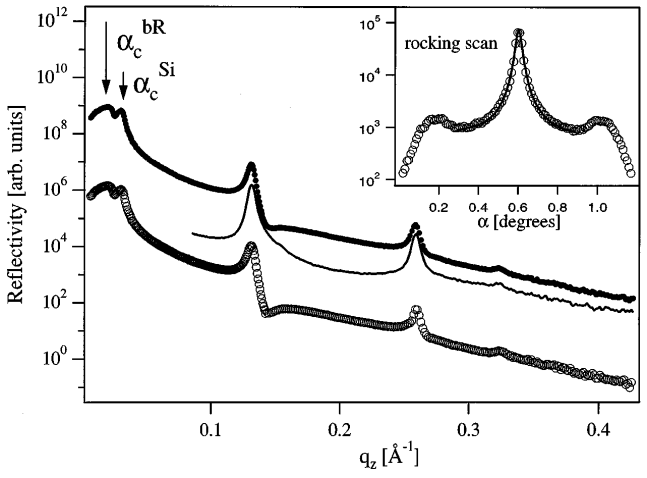

FIG. 2. Reflectivity (solid circles), offset (line), and true specular (open circles) scans of dry bR multilayer of fused patches. Inset shows rocking scan, where the solid line is a Lorentzian fit to the central specular part (FWHM = 0.4°). Arrows point to critical angles for bR and Si.

wings at $\alpha_{i/f} = \alpha_c$ [9]. Diffuse scattering is also apparent in the offset scan (Fig. 2, solid line) done with an offset angle of $\Delta\alpha = 0.2°$ with respect to the specular direction. From the positions of the Bragg peaks, the repeat distance of the multilayer 49 Å, corresponding to just one layer of water between the membranes (membrane thickness is $\delta_m = 47$ Å). Hydrating the multilayer sample to a membrane repeat spacing of 66.9 Å (20 Å water between membranes) did not affect the quality of alignment in the sample. The specular reflectivity curve (Fig. 2, open circles) was obtained by subtracting the offset scan from the reflectivity profile. In the Born approximation the specular reflectivity profile may be characterized by the expression [10]

$$R(q_z) = R_F(q_z) \left| \frac{1}{\rho_0} \int \frac{d\rho(z)}{dz} e^{iq_z z} \right|^2,$$

were $R_F(q_z)$ is the Fresnel reflectivity and ρ_0 is the mean electron density of the sample. It is a measure of the projected electron density $\rho(z)$ along the average membrane normal direction. Extension of this method to other protein-rich membranes, such as bacterial S-layers [2] or gap junctions would give valuable insight to the yet unknown structure of those proteins.

The highly ordered fused patch samples allow quantitative diffuse scattering measurements to be done on protein-rich membranes. These measurements are sensitive to lateral inhomogeneities and membrane corrugations. Indeed, the offset scan shows significant diffuse scattering enhanced near Bragg peaks, the so-called diffuse Bragg sheets [11]. This is indicative of a coherent interference of scattering in neighboring layers, i.e., of in-plane disorder that is strongly correlated normal to the layers. From thickness of the Bragg sheets, a vertical correlation length of more than 3000 Å is inferred, compared to the estimated film thickness of 1 μm.

There are several possible sources of diffuse scattering. Density fluctuations due to long-wavelength phonons can be excluded since (i) they are not expected to be correlated across many layers, especially since we have found that the proteins in neighboring layers are not positionally correlated (see below), and (ii) they would have a long range cutoff only at very high values determined by the size of the crystalline domains. The latter is inconsistent with a well-separated specular and diffuse component, as is evidenced in rocking scans. We can also exclude static density fluctuations with lateral length scales of a few hundred angstroms, because in-plane density fluctuations must lead to a characteristic decay of diffuse intensity $S(q_\parallel \approx 0, q_z)$ with q_z [12], given by the form factor of 1 layer modulated by Bragg sheets. It would be nearly constant on the semilogarithmic scale up to $2\pi/\delta_m$ and then fall off faster than algebraically. Instead, an average power-law decay (again modulated by the Bragg sheets) of q_z^{-4} is in good agreement with the data.

The observed diffuse scattering enhanced in the Bragg sheets is consistent with a conformal membrane corrugation. For a self-affine surface the height-height difference

function $g(|\mathbf{r}|) = \langle [z(0) - z(\mathbf{r})]^2 \rangle$ is given by $g(|\mathbf{r}|) \propto r^{2h}$ for $r \ll \xi$, where ξ is the correlation length and h the so-called roughness exponent. It can be shown that the structure factor at fixed small $q_\parallel$ decays as $S(q_\parallel \approx 0, q_z) \propto 1/q_z^{(2/h+2)}$ [9]. Thus, in the present case we deduce a membrane roughness with an exponent around $h \sim 1$, which means that the surface is smooth on length scales smaller than ξ.

The in-plane structure (i.e., the height difference function) is more sensitively probed by investigating the diffuse scattering as a function of lateral momentum transfer [12]. The two-dimensional intensity distribution as a function of q_z and $q_\parallel$, measured in an out-of-plane geometry where refraction effects do not distort the scattering distribution, is shown in the contour plot of Fig. 3(a). A striking feature is the distribution of diffuse scattering along an arc in the $(q_\parallel, q_z)$ plane (dashed line). This is not an effect of bad mosaicity, since the central width of the mosaicity distribution of less than 0.04° is evident from the rocking scan, so that membrane layers are macroscopically well aligned. We therefore attribute the diffuse Bragg sheet bend to a distribution of tilt angles γ of the local membrane orientation, resulting in a maximum replication (conformality) in directions offset with respect to the q_z axis, e.g., corresponding to the simple real space schematic of the inset of Fig. 3(a). In other words, the tilt of the Bragg sheet can be explained by a local faceting or buckling of the membrane with a distribution of tilt angles of the facets of $\Delta\gamma = 4.6°$. To further investigate this possibility, we plot the integrated intensity of the Bragg sheet as a function of $q_\parallel$ [Fig. 3(b)], where as a result of the q_z integration, the cross correlations drop out and the lateral structure factor of an averaged single interface is obtained. The broad peak at small $q_\parallel$ is followed by a very strong decay that saturates at about 0.1 Å^{-1} at an intensity 4 orders of magnitude below the peak, before it slightly increases again close to the tail of the hexagonal (10) peak. The monotonic decay indicates the absence of any well-defined lateral length scale, but the position marked by the arrow can be taken to define a correlation length ξ of about 300 Å, which corresponds to the lateral length scale of the corrugation (~6 protein lattice units). The membrane cannot have any random roughness on length scales smaller than ξ. Indeed, using a recently established back transformation of $S(q_\parallel)$ [13], the height difference function $g(r)$ can be computed with no adjustable parameters in a model-independent manner [14]. The resulting function $g(r)$ is plotted in Fig. 3(c). For $r \ll \xi$, $g(r)$ increases with a roughness exponent $h \approx 0.9$. The height difference increases almost linearly with the distance r between two points, which is the prediction for a locally flat but inclined interface. Within experimental error this result is in agreement with the conclusion drawn from the $S(q_z, q_\parallel = 0) \propto q_z^{-4}$ dependence.

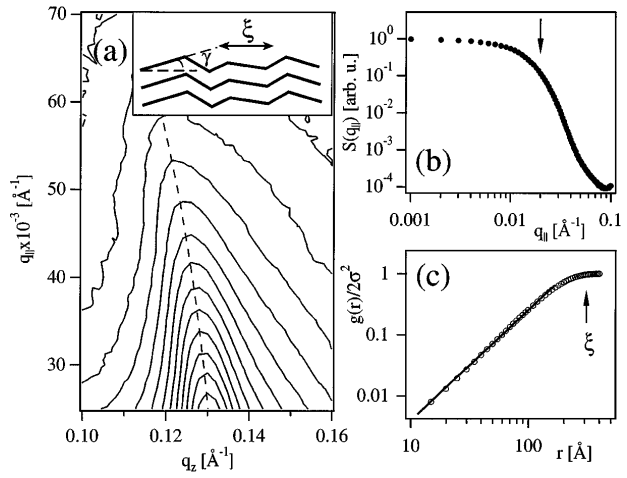

FIG. 3. (a) Distribution of diffuse scattering intensity of the first Bragg sheet. Inset shows a possible real-space picture of conformal membrane corrugation consistent with the measured diffuse scattering; (b) $S(q_\parallel)$ integrated over q_z on a double-logarithmic scale; (c) height-height correlation function obtained from $S(q_\parallel)$; solid line is a fit with $h = 0.905$.

Purple membrane multilayers approximate a stack of decoupled crystalline membranes, which should exhibit significant diffuse scattering because of thermal fluctuations [15]. However, the diffuse scattering along $q_\parallel$ in Fig. 3(b) decays faster than predicted for the fluctuating membranes, which should exhibit a power-law decay with a slope ≤ 4 with a long-wavelength cutoff determined by the lattice domain size (a few μm in our case), rather than by a correlation length of 300 Å. Thus, a possible contribution of thermal undulations of crystalline membranes to the diffuse scattering is completely dominated in our system by the contribution from the conformal membrane corrugation. Since the measured correlation length $\xi \sim 300$ Å is smaller than the native PM patch size of ~5000 Å, the corrugation is not caused by the residual defects introduced by the fusion process. It must be caused by the presence of the protein lattice in the membrane, since the PM lipids are always fluid and therefore unlikely to pack in any preferred way.

In order to investigate possible correlations between the proteins in neighboring membranes, we have measured the truncation rods of the 2D protein crystals. These are scans along the q_z direction with $q_\parallel$ fixed at the position of an in-plane protein lattice peak. The Bragg rod for a single crystalline domain may be described by

$$I_{hk}(q_z) \propto |V(q_z)F(\mathbf{G}_{hk}, q_z)|^2 S(\mathbf{G}_{hk}, q_z)\,.$$

Here $V^2(q_z)$ is the Fresnel transmission function for the incident beam, $F(\mathbf{G}_{hk}, q_z)$ and $S(\mathbf{G}_{hk}, q_z)$ are form factor and structure factor, respectively. $S(\mathbf{G}_{hk}, q_z)$ reflects any correlations between the proteins in different membranes. $F(\mathbf{G}_{hk}, q)$ is the out-of-plane form factor of protein molecule. Because of the in-plane random orientations of the many single-crystalline fused membrane patches illuminated by an x-ray beam, the normal truncation rods in reciprocal space become concentric cylinders with the

cylinder axis along the out-of-plane (q_z) direction. The rod scan of the (11) lattice peak is shown in Fig. 4(a). The measurement was done for a dehydrated sample and for a hydrated sample at RH = 95% (d = 66.9 Å). Two features of these scans are immediately apparent: (i) there are no long-range positional correlations between the proteins in adjacent layers at either hydration level, since the presence of such correlations would manifest itself in sharp modulations of the rods; (ii) the rod of the hydrated sample is distinctly different from the rod of the dry one. Correcting the rod of hydrated sample by the Fresnel transmission function, we obtain the true rod scan shown in Fig. 4(b). The resulting curve is simply a form factor of the protein $|F(\mathbf{G}_{11}, q_z)|^2$. Therefore, in the hydrated case the proteins in different membranes have no positional locking at all: $S(G_{11}, q_z) = \text{const}$. Dividing the rod scan of dehydrated multilayer by $|F(\mathbf{G}_{11}, q_z)|^2$ should yield the structure factor $S(\mathbf{G}_{11}, q_z)$ of the protein packing between the different membranes. This is shown in Fig. 4(c). The structure factor peaks at 0.12 Å^{-1} with peak width of $\sim$0.1 Å^{-1}. We attribute this broad interlayer protein correlation peak to the lock-in of the hexagonal lattices in neighboring membranes in a random ABC...-type repeat sequence. This is indeed plausible since the proteins protrude from the lipid membrane by $\sim$2 Å. The possibility of three different (A,B,C) lock-in configurations between hexagonal layers explains the random packing with no long-range order, thus giving only a broad correlation peak in the structure factor.

We emphasize that the short-range locking occurs only in completely dehydrated samples. This result may be important in explaining the anomalously high thermal denaturation temperature (140 °C) of bacteriorhodopsin in dry multilayers [16]. Since it is likely that bR unfolds out of the bilayers into the intermembrane space during the thermal denaturation transition [17], the observed locking would stabilize the proteins by simply eliminating the available space into which they unfold. This is consistent with the absence of melting transition of the bR crystalline lattice in the dehydrated multilayers, because the locked-in lattices are likely to be more stable than the decoupled ones.

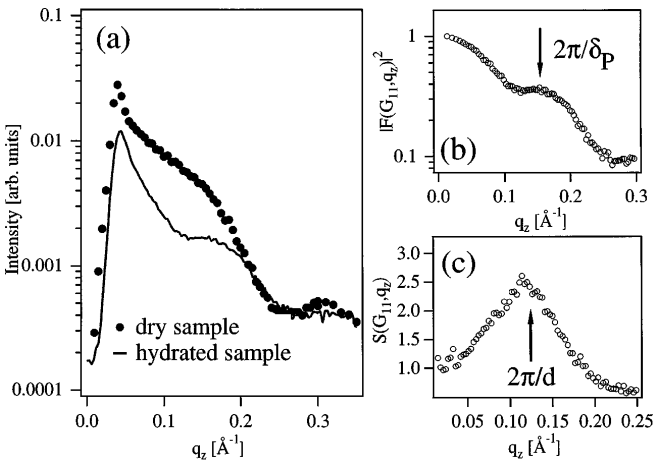

FIG. 4. (a) Comparison of the (11) rod scans of dry (solid circles) and hydrated (solid line) multilayers; (b) protein form factor obtained from the hydrated multilayer rod scan. Arrow indicates the peak due to protein thickness δ_p; (c) structure factor for protein correlations in dehydrated multilayer.

In conclusion, we have presented the first study of specular and diffuse reflectivity from a multilayer of native biological membranes containing integral membrane proteins, where the analysis of membrane conformations and protein-protein correlations becomes simple and unambiguous. This experimental approach can provide insight into the multilayers of other membrane proteins (e.g., S-layers [2]) even before a complete crystallographic solution of their structure.

We thank G. C. L. Wong for critically reading the manuscript. This work was supported by NSF DMR-9624091 and PRF-31352-AC7. C. R. S. acknowledges financial support from the Curie Institute and T. S. from the DAAD.

*Present address: Sektion Physik der Ludwig-Maximilians-Universitat Munchen, Munchen, Germany.

[1] H. Lodish *et al.*, *Molecular Cell Biology* (Scientific American Books, New York, 1995).
[2] W. Baumeister and G. Lembcke, J. Bioenerg. Biomembr. **24**, 567 (1992).
[3] *Nanofabrication and Biosystems*, edited by H. C. Hoch, L. W. Jelinski, and H. G. Craighead (Cambridge University Press, Cambridge, 1996).
[4] R. R. Birge, Sci. Am. **272**, 90 (1995).
[5] *Structure and Dynamics of Membranes*, edited by R. Lipowsky and E. Sackmann (Elsevier Science, New York, 1995).
[6] G. S. Smith, E. B. Sirota, C. R. Safinya, and N. A. Clark, Phys. Rev. Lett. **60**, 813 (1988).
[7] J. Baldwin and R. Henderson, Ultramicroscopy **14**, 319 (1984); R. Henderson *et al.*, J. Mol. Biol. **213**, 899 (1990).
[8] A. E. Blaurock, J. Mol. Biol. **93**, 139 (1975).
[9] S. K.Sinha, E. B. Sirota, and S. Garoff, Phys. Rev. B **38**, 2297 (1988).
[10] A. Braslau *et al.*, Phys. Rev. A **38**, 2457 (1988).
[11] T. Salditt, T. H. Metzger, and J. Piesl, Phys. Rev. Lett. **73**, 2228 (1994).
[12] M. Rauscher, T. Salditt, and H. Spohn, Phys. Rev. B **52**, 16 855 (1995).
[13] T. Salditt *et al.*, Europhys. Lett. **32**, 331 (1995).
[14] $g(r)$ can be obtained from $S(q_\parallel)$ if the rms roughness σ is known by an inverse Hankel transform in Eq. [2.28(b)] in Ref. [9]. We estimate σ to be 7 Å from the decay of the integrated intensities of the multilayer Bragg peaks. The roughness exponent h is rather insensitive to the errors in σ.
[15] T. Toner, Phys. Rev. Lett. **64**, 1741 (1990); H. S. Seung and D. R. Nelson, Phys. Rev. A **38**, 1005 (1988).
[16] Y. Shen *et al.*, Nature (London) **366**, 48 (1993).
[17] I. Koltover and C. R. Safinya (to be published).